COMPUTATIONAL METHODS (EP208)
PROJECT REPORT

NEONATAL HYPERTHERMIA

THE DEVELOPMENT OF REAL TIME MONITORING SYSTEM TO PREVENT HYPERTHERMIA IN SEVERE CASES OF HYPERBILIRUBINEMIA

SUBMITTED BY:

KREETY KHATRI - 2K19/EP/045
PULKIT PANDEY – 2K19/EP/076

DEPARTMENT OF APPLIED PHYSICS

DELHI TECHNOLOGICAL UNIVERSITY, NEW DELHI, 110042, INDIA

ACKNOWLEDGEMENT

Presentation, Inspiration and Motivation have always played a key role in success of any project.

We express a deep sense of gratitude to **Dr AJEET KUMAR, Assistant Professor, Department of Applied Physics, DTU** to encourage us to highest peak and to provide with the opportunity to prepare the project. We are immensely obliged to him for his elevating inspiration, encouraging guidance and kind supervision in the completion of the project.

We are also thankful for his invaluably constructive criticism and advises throughout the working of the project. The accomplishment of the project was due to our sole efforts and contribution. We are highly indebted towards our University, that is, Delhi Technological University, New Delhi

CONTENTS

I - PREFACE

ABSTRACT~ Neonatal jaundice also known as hyperbilirubinemia is a phenomenon that occurs in 60% of all term new-borns. Severe cases of this may lead to chronic encephalopathy, kernicterus, neurologic deficits, and, in some cases, death. Intensive blue light phototherapy involves irradiation of a patient with high intensity light and is widely used for treatment of severe hyperbilirubinemia. As a result, Hyperthermia occurs in some neonates during intensive blue light phototherapy. Body temperature of a hypothetical neonate undergoing intensive blue light phototherapy is mathematically modelled to investigate parameters that cause hyperthermia.

The objective of fabricating this project is to illuminate the concept of Computational Methods in solving the bio heat transfer equation to develop a real time monitoring system that may be used to prevent Hyperthermia in neonates using the developed model. This document presents the detailed analysis undertaken to analyse the change in transient temperature of human neonate undergoing phototherapy to treat the condition of hyperbilirubinemia and investigating the parameters that may be used to detect the real cause of Hyperthermia.

BILIRUBIN~ Bilirubin (BR) is a yellow compound that occurs in the normal catabolic pathway that breaks down heme. This catabolism is a necessary process in the body's clearance of waste products that arise from the destruction of aged or abnormal red blood cells (RBCs). First the hemoglobin gets stripped of the heme molecule which thereafter passes through various processes of catabolism, depending on the part of the body in which the breakdown occurs. It's hard for babies to get rid of bilirubin at first. It can build up in their blood, tissues, and fluids. Bilirubin has a color. It makes a baby's skin, eyes, and other tissues turn yellow (jaundice). Jaundice may first appear when your baby is born. Or it may also show up any time after birth.

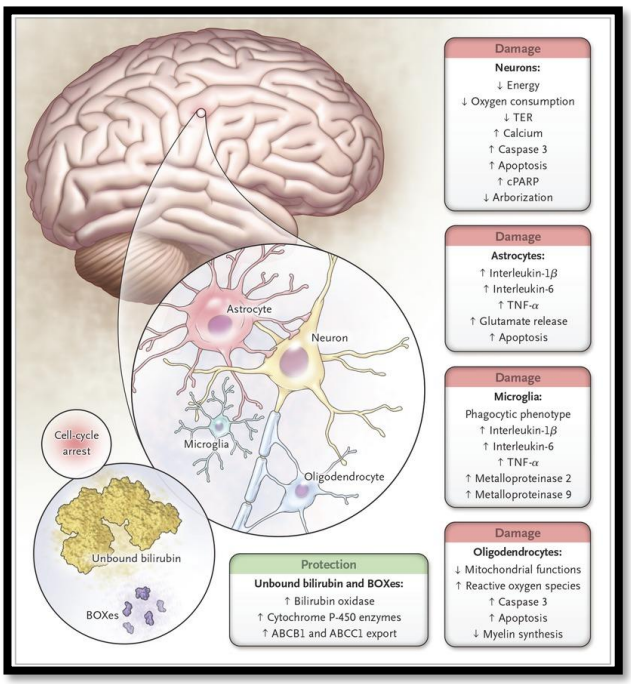

FIGURE - 1

BLOOD PERFUSION RATE~ Perfusion is the passage of fluid through the circulatory system or lymphatic system to an organ or a tissue, usually referring to the delivery of blood to a capillary bed

in tissue. Perfusion is measured as the rate at which blood is delivered to tissue, or volume of blood per unit time (blood flow) per unit tissue mass. The SI unit is $m^3/(s \cdot kg)$, although for human organs perfusion is typically reported in ml/min/g.

HEAT TRANSFER~ When the environment is not thermoneutral, the body uses four mechanisms of heat exchange to maintain homeostasis: conduction, convection, radiation, and evaporation. Each of these mechanisms relies on the property of heat to flow from a higher concentration to a lower concentration; therefore, each of the mechanisms of heat exchange varies in rate according to the temperature and conditions of the environment.

CONDUCTION~ It is the transfer of heat by two objects that are in direct contact with one another. It occurs when the skin comes in contact with a cold or warm object. For example, when holding a glass of ice water, the heat from your skin will warm the glass and in turn melt the ice. Alternatively, on a cold day, you might warm up by wrapping your cold hands around a hot mug of coffee. Only about 3 percent of the body's heat is lost through conduction.

CONVENTION~ It is the transfer of heat to the air surrounding the skin. The warmed air rises away from the body and is replaced by cooler air that is subsequently heated. Convection can also occur in water. When the water temperature is lower than the body's temperature, the body loses heat by warming the water closest to the skin, which moves away to be replaced by cooler water. The convection currents created by the temperature changes continue to draw heat away from the body more quickly than the body can replace it, resulting in hyperthermia. About 15 percent of the body's heat is lost through convection.

RADIATION~ It is the transfer of heat via infrared waves. This occurs between any two objects when their temperatures differ. A radiator can warm a room via radiant heat. On a sunny day, the radiation from the sun warms the skin. The same principle works from the body to the environment. About 60 percent of the heat lost by the body is lost through radiation.

EVAPORATION~ It is the transfer of heat by the evaporation of water. Because it takes a great deal of energy for a water molecule to change from a liquid to a gas, evaporating water (in the form of sweat) takes with it a great deal of energy from the skin. However, the rate at which evaporation occurs depends on relative humidity—more sweat evaporates in lower humidity environments. Sweating is the primary means of cooling the body during exercise, whereas at rest, about 20 percent of the heat lost by the body occurs through evaporation.

BASAL METABOLIC RATE~ The metabolic rate is the amount of energy consumed minus the amount of energy expended by the body. The basal metabolic rate (BMR) describes the amount of daily energy expended by humans at rest, in a neutrally temperate environment, while in the postabsorptive state. It measures how much energy the body needs for normal, basic, daily activity. About 70 percent of all daily energy expenditure comes from the basic functions of the organs in the body. Another 20 percent comes from physical activity, and the remaining 10 percent is necessary for body thermoregulation or temperature control.

II - HYPERBILIRUBINEMIA IN HUMAN NEONATE

BACKGROUND THEORY

Unconjugated 4Z,15Z-bilirubin is a toxic and insoluble product of heme-catabolism that does not readily exit the body. Bilirubin leaves the body after binding to glucuronic acid in the liver to form a water soluble compound (i.e. conjugated bilirubin), which can be excreted into the bile. Blood vessels transport unconjugated bilirubin to the liver as bilirubin bound to albumin. Bilirubin dissociates from albumin in the liver, is rapidly internalized by hepatocytes, and binds to ligandin molecules inside the cells. Bilirubin and glucuronic acid conjugate in a reaction catalyzed by diphosphoglucuronyltransferase (UDPGT).

Indirect hyperbilirubinemia is defined as an abnormally elevated concentration of unconjugated bilirubin in the blood. Neonatal hyperbilirubinemia occurs in the majority of newborns. Two concurrent factors contribute to this prevalence. Firstly, fetal erythrocytes are rapidly broken down shortly postpartum, resulting in a rapid production of unconjugated bilirubin. Secondly, ligandin concentration and UDPGT activity are both below mature levels in the neonatal liver. Neonates with congenital liver disease, such as Gilbert Syndrome, are at an increased risk for severe hyperbilirubinemia. Severe hyperbilirubinemia can cause chronic brain damage. Unconjugated bilirubin in the blood can transcend the blood brain barrier and accumulate in the central nervous system (CNS). Slightly more than half of all neonates become visibly jaundiced in the first week of life. Almost all hyperbilirubinemia in the immediate neonatal period is unconjugated, which is termed indirect bilirubin, based on older laboratory measurement methods; conjugated bilirubin is termed direct bilirubin.

Accumulation of bilirubin in the CNS can lead to permanent brain lesions, resulting in long-term neurologic disease and possibly death.

➢ PHYSIOLOGIC JAUNDICE

It occurs in almost all neonates. Shorter neonatal red blood cell life span increases bilirubin production, deficient conjugation due to the deficiency of uridine diphosphate-glucuronosyltransferase (UGT) decreases clearance, and low bacterial levels in the intestine combined with increased hydrolysis of conjugated bilirubin increase enterohepatic circulation. Bilirubin levels can rise up to 18 mg/dL (308 micromol/L) by 3 to 4 days of life (7 days in Asian infants) and fall thereafter.

➢ BREAST FEEDING FAILURE JAUNDICE

Breastfeeding jaundice develops in one sixth of breastfed infants during the first week of life. Breastfeeding increases enterohepatic circulation of bilirubin in some infants who have decreased milk intake and who also have dehydration or low caloric intake. The increased enterohepatic circulation also may result from reduced intestinal bacteria that convert bilirubin to nonresorbed metabolites.

➢ BREAST MILK JAUNDICE

Breast milk jaundice is different from breastfeeding jaundice. It develops after the first 5 to 7 days of life and peaks at about 2 weeks. It is thought to be caused by an increased concentration of beta-glucuronidase in breast milk, causing an increase in the deconjugation and reabsorption of bilirubin.

➢ PATHOLOGICAL JAUNDICE

Pathologic hyperbilirubinemia in term infants is diagnosed if

- Jaundice appears in the first 24 hours, after the first week of life, or lasts > 2 weeks
- Total serum bilirubin rises by > 5 mg/dL/day (> 86 micromol/L/day)
- Total serum bilirubin is > 18 mg/dL (> 308 micromol/L/day)
- Infant shows symptoms or signs of a serious illness

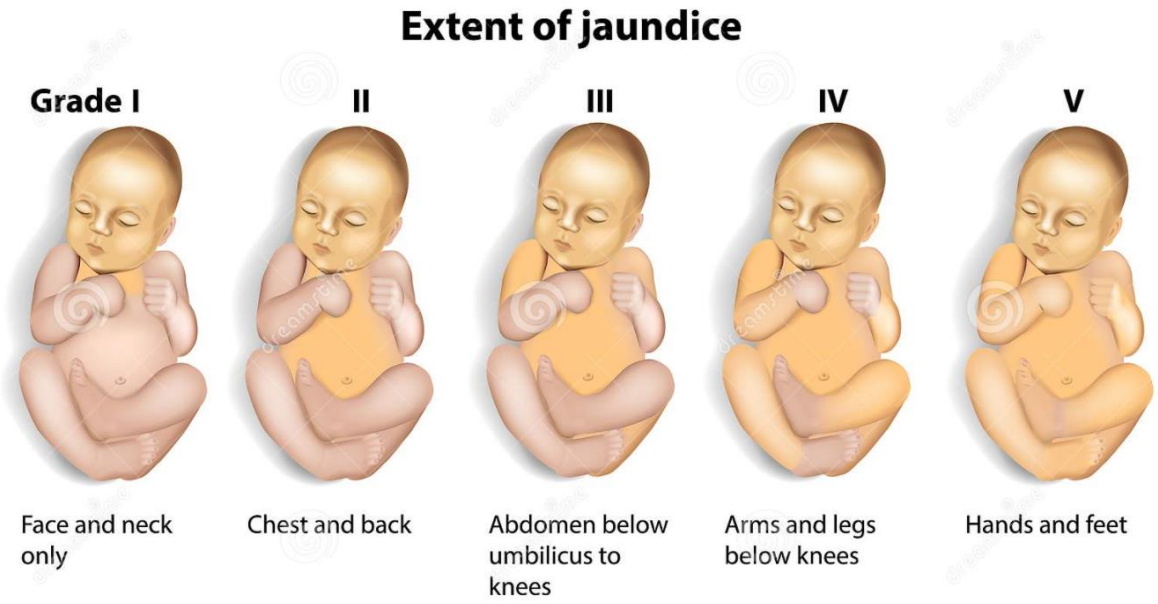

FIGURE - 2

III - FUNDAMENTALS OF PHOTOTHERAPY

Phototherapy is the use of visible light for the treatment of hyperbilirubinemia in the new born. This relatively common therapy lowers the serum bilirubin level by transforming bilirubin into water-soluble isomers that can be eliminated without conjugation in the liver. The dose of phototherapy is a key factor in how quickly it works; dose in turn is determined by the wavelength of the light, the intensity of the light (irradiance), the distance between the light and the baby, and the body surface area exposed to the light. Commercially available phototherapy systems include those that deliver light via fluorescent bulbs, halogen quartz lamps, light-emitting diodes, and fiber-optic mattresses. Proper nursing care enhances the effectiveness of phototherapy and minimizes complications. Caregiver responsibilities include ensuring effective irradiance delivery, maximizing skin exposure, providing eye protection and eye care, careful attention to thermoregulation, maintaining adequate hydration, promoting elimination, and supporting parent-infant interaction

➢ WORKING OF PHOTOTHERAPY

Phototherapy converts bilirubin that is present in the superficial capillaries and interstitial spaces of the skin and subcutaneous tissues to water-soluble isomers that are excretable without further metabolism by the liver. Neonatal jaundice expert Maisels suggests that phototherapy is much like a percutaneous drug. When phototherapy illuminates the skin, an infusion of discrete photons of energy are absorbed by bilirubin much like a drug molecule binds to a receptor. Bilirubin molecules in light-exposed skin undergo relatively quick photochemical reactions—configurational isomerization, structural isomerization, and photooxidation—to form nontoxic, excretable isomers. These bilirubin isomers have different shapes than the native isomer, are more polar, and can be excreted from the liver into the bile without undergoing conjugation or requiring special transport for their excretion. Urinary and gastrointestinal elimination remain important to the process of reducing the bilirubin load.

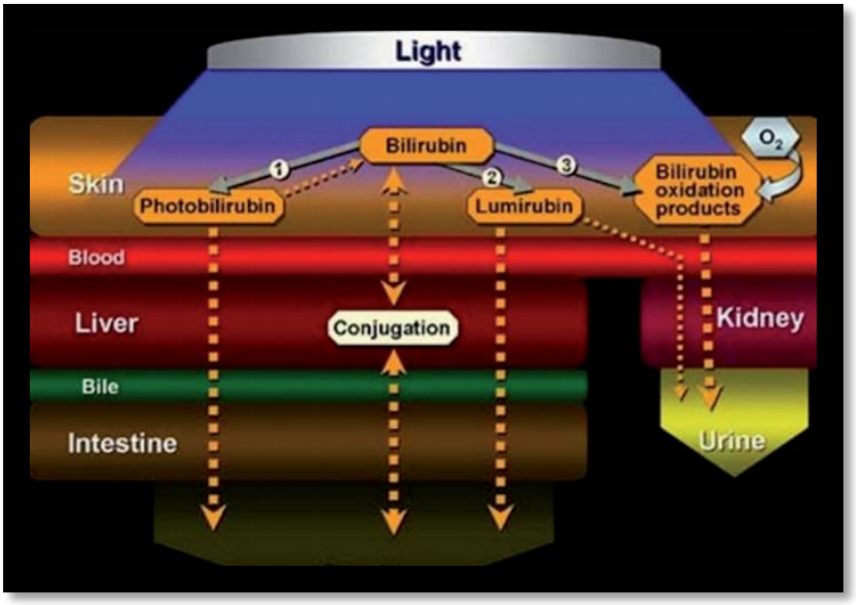

FIGURE -3

➢ THE IMPORTANCE OF DOSE

A robust relationship exists between the dose of phototherapy and the rate of decline in serum bilirubin level. Dose of phototherapy is determined by several key factors:

• ***Spectral qualities of the light source used (wavelength range and peak);***

The most effective light sources for degrading bilirubin emit light in a relatively narrow wavelength range (400 to 520 nanometers, or nm), with a peak of 460 -510 nm. At these wavelengths, light penetrates the skin well and is maximally absorbed by bilirubin. Blue, green, and turquoise light (the blue-green spectrum) are considered the most effective, and some evidences suggest that given equal irradiance levels, the turquoise spectral range is more efficient in reducing bilirubin than blue because of greater skin penetration.

• ***Intensity of the light (irradiance);***

Irradiance is the light intensity, or number of photons delivered per square centimeters of exposed body surface. The delivered irradiance determines the effectiveness of phototherapy; the higher the irradiance, the faster the decline in serum bilirubin level. Spectral irradiance, quantified as W/cm2/nm, varies with the design of the light source. It can be measured with a spectral radiometer sensitive to the effective wavelength of light. Intensive phototherapy requires a spectral irradiance of 30 W/cm2/nm, delivered over as much of the body surface as possible.

• ***Distance between the light and the infant's skin;***

Light intensity is inversely related to the distance between the light and the body surface. A simple way to increase irradiance is to move the light closer to the infant. Caution must be exerted when positioning halogen phototherapy lamps, which cannot be positioned closer to the infant than recommended by their manufacturers without incurring the risk for a burn.

• ***Body surface area exposed by the irradiated field or "footprint."***

The greater the body surface area exposed to light, the faster the decline in serum bilirubin. Many light sources used in neonatal care do not expose a sufficient area of skin to the light. The light source may have an adequate spectral irradiance in the centre of the light's footprint; however, irradiance decays significantly at the periphery of the light.The result is that only an insufficient proportion of the infant's body surface area receives effective treatment. This problem can be solved by positioning the infant properly within the footprint of the light or using multiple light sources for coverage of at least 80% of the body surface.

The size of the exposed body surface area, along with the level of irradiance, determines the spectral power of the phototherapy application, which in turn influences its effectiveness.The larger the exposed body surface and stronger the light, the higher the spectral power

➢ LIMITATIONS OF PHOTOTHERAPY

The irradiance and surface area exposure produced by home phototherapy units are lower than those produced by typical hospital making them less efficient at lowering the serum bilirubin level. Whether a valid indication for home phototherapy exists is questionable; current guidelines state that a bilirubin high enough to warrant treatment should be managed in the hospital. In the past, parents have sometimes been told to expose their jaundiced infants to sunlight. Notwithstanding phototherapy's beginnings in the sunny courtyard of an English hospital, this practice is not considered a safe or reliable way to treat jaundice. There are reports in the literature of infants developing kernicterus after their parents were instructed to treat their infants' jaundice at home by exposing them to sunlight, in some cases for as little as 15 minutes per day. Not only was this very likely to be ineffective but also it probably contributed to hyperbilirubinemia as well as delays in proper treatment.

The most noticeable clinical complication of phototherapy is "bronze baby syndrome," a grayish-brown discoloration of the skin that occurs exclusively in infants with cholestatic jaundice. Bronze baby syndrome is believed to occur when the brown photoproducts of porphyrins, especially copper porphyrins, accumulate in the skin and their excretion is impaired by cholestasis. Phototherapy can damage red-blood-cell membranes, increasing their susceptibility to lipid peroxidation and hemolysis. These effects may contribute to the pathogenesis of disorders common in the very low-birth-weight infant, including bronchopulmonary dysplasia, retinopathy of prematurity, and necrotizing enterocolitis. Due to high intensive phototherapy, it can leads to hyperthermia in neonates which is prime focus of this report.

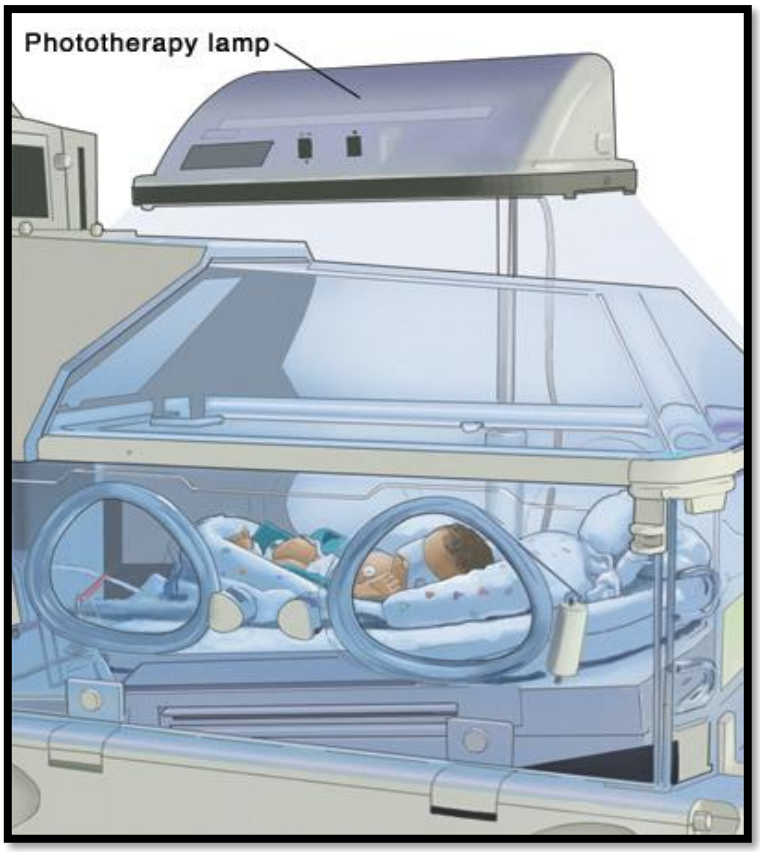

FIGURE - 4

IV- MATHEMATICAL MODEL OF HUMAN NEONATE

➢ PHYSICAL SYSTEM AND SURROUNDINGS

The development of the model begins by simplifying the neonate geometry, assigning physical quantities to each tissue group, assuming an initial temperature profile and describing the neonate's surroundings. The geometry of a supine neonate body is simplified to a single circular cylinder. The total mass of the cylinder is set equal to 3.2 kg, the average mass of a neonate. The average height of a neonate is 0.50 m. The body surface area (BSA) of the average neonate is approximated by inputting the previously stated values of height and mass into the lateral surface formula. The value of this is 0.21 m^2 and is set equal to the lateral surface area of the cylinder. Dividing the total mass of the cylinder by the average density of a neonate gives the total volume of the cylinder, equal to 3100 cm^3. The volume and lateral surface area of the cylinder are used to calculate its length and the cross sectional radius. These are 1.1 m and 3 cm, respectively.

The cylinder is divided into six parts, a central cylinder circumscribed by five shells. Each part represents a different tissue type within the simplified neonate body. It is assumed that there is perfect thermal contact between each tissue group and the tissue groups adjacent to it. The body parts considered here and in other thermal models of the human body are the cortex, brain stem, cervical medulla, thoracic medulla, liver, kidney, stomach, gut, bladder, thyroid gland, spleen, oesophagus, trachea, lungs, heart, blood, bone, muscle, connective tissue, fat and skin. The mass fractions of bone, muscle, connective, fat and skin tissue are higher than for other body parts, and these tissues are closest to the surface of the body per data obtained by others.

Each of these is represented by one of the shells separating the central cylinder from the surroundings. The bone shell is in direct contact with the central cylinder and is surrounded by muscle, connective, fat, and skin tissue, mentioned in the order of increasing distance from the central cylinder. A thermal model done by Ferreira and Yanagihara uses a similar configuration.

The volume of each shell is calculated by multiplying the volume fraction of the tissue that shell represents by the total volume of the simplified neonatal body. The remaining body parts are labeled core structures. These are represented by the central cylinder, which is composed of a hypothetical tissue type labeled "core tissue". The change in core tissue temperature approximates the average change in temperature of core structures within the body. The volume of the central cylinder is equal to the sum of the volume fractions of each body part represented by the central cylinder multiplied by the total volume of the simplified neonatal body. The mass weighted mean of each physical property pertinent to the model is averaged over all body parts that make up the core and set equal to the value of that physical property in the core tissue. The radius of the central cylinder and the outer radius of each shell is calculated using the volume of each shell and the length of the body. The experimentally determined value of density and specific heat capacity of blood are also used when evaluating convective heat exchange between the tissue and blood.

All tissue groups are assumed to be at an initial temperature of 37 °C. The simplified neonate body lays in a hypothetical incubator on top of a blanket. The blanket covers half the BSA. The incubator walls surround the body. The air inside the incubator is saturated with water. The temperature of the blanket, walls, and air is set to a constant 33 °C, equal to the average temperature of a neonate

incubator during blue light phototherapy measured in the clinical setting. Matter outside the incubator is not considered. A source of blue light exists above the cylinder and irradiates the top half of the cylinder with light in the 430-490 nm spectrum (the region of blue light used in the definition of intensive blue light phototherapy put forth by the APA) at a constant spectral irradiance. No other sources of visible light are present. The blue light source is far from the infant, and non-radiative heat generated by the light source is not considered.

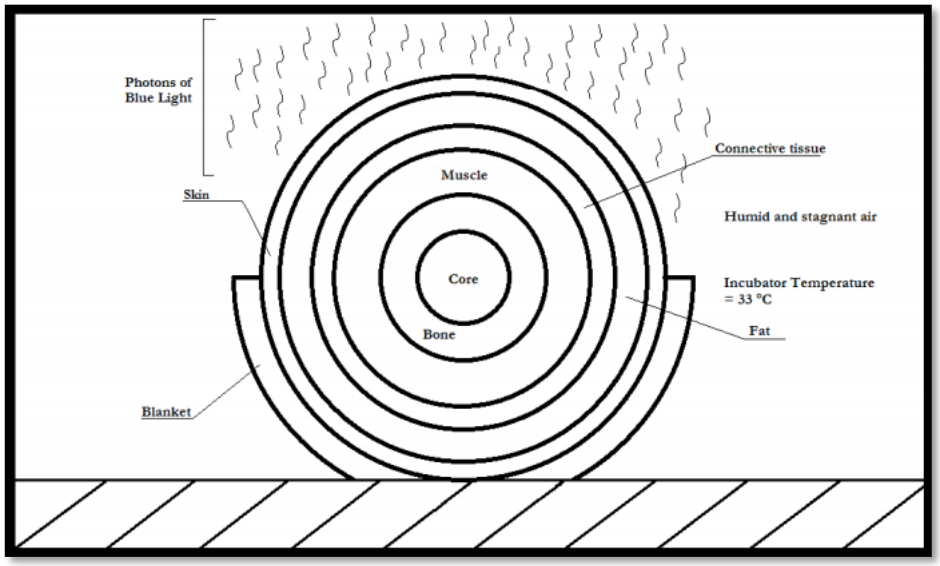

FIGURE-5

EXPERIMENTALLY DETERMINED VALUES

Tissue Type	Volume [cm^3]	Outer Radius [cm]	Density [kg/m^3]	Specific Heat Capacity [J/kg-K]
Core	471	1.2	970	3650
Bone	372	1.6	1520	1700
Muscle	1400	2.5	1085	3800
Connective	214	2.6	1085	3200
Fat	502	2.9	920	2300
Skin	164	3	1085	3680
Blood	-	-	1059	3850

FIGURE-6

Tissue Type	Thermal Conductivity [W/m-K]	Basal Blood Perfusion Rate [m^3_{blood}/m^3_{tissue} x 10^6]	Basal Metabolic Heat Production [W/m^3]
Core	0.47	1800	828
Bone	0.65	0	368
Muscle	0.51	543	684
Connective	0.47	100	369
Fat	0.21	77	300
Skin	0.47	362	368

FIGURE-7

➢ GENERAL MODEL DEVELOPMENT

The goal of this section is to develop a differential equation describing temperature variation within the simplified neonate body as a function of time and position. The development focuses on an arbitrary point and is generalizable to any point within the body. An arbitrary point in the body is treated as a closed thermodynamic system. The temperature of the system relates to its internal energy. Change in internal energy over time is equal to the net rate of heat entering the system and the net rate of work done on the system. This equivalence is an energy balance derived from the first law of thermodynamics. Its mathematical form is:

$$\frac{dU}{dt} = H + W$$

where dU is change in internal energy, dt is change in time, H is net rate of heat entering the system and W is net rate of work done on the system. The following assumptions are applied: work is not done, bulk kinetic energy is constant, and potential energy is constant. Considering these, the specific heat formula relates change in temperature to change in internal energy. Applying the stated assumptions and incorporating the specific heat formula into the energy balance gives:

$$\frac{d(m * C_P * T)}{dt} = H$$

where m is mass, Cp is specific heat, and T is temperature. The temperature at a single point in the body is assumed to be independent of longitudinal position and azimuth angle. Assuming this, the energy balance taken around a single point is equivalent to an energy balance taken around an infinitesimally thin shell that encompasses that point and that extends down the central axis of the cylindrical body. The remainder of the development considers the energy balance taken around the thin shell. Applying equation 1.2 to the shell, the value of H is equal to the net rate of heat entering and leaving the shell and the net rate of heat generated and consumed within the shell. Qualitatively incorporating this into the energy balance gives:

$$\frac{d(m * C_P * T)}{dt} = Heat_{\,(In-Out)} + Heat_{\,(Generation-Consumption)}$$

Net basal metabolic heat production (B) multiplied by the volume (V) of the shell gives the net heat generated and consumed within the shell. B is assumed constant, recalling that biologic processes possibly triggered during phototherapy are not considered here.

$$Heat_{\,(Generation-Consumption)} = B * V$$

Heat enters and leaves the shell via convective, radiative and conductive heat transfer. It is assumed that heat transfer does not occur at the circular ends of the cylindrical body.

$$Heat_{\,(In-Out)} = Convective\ HT + Radiative\ HT + Conductive\ HT$$

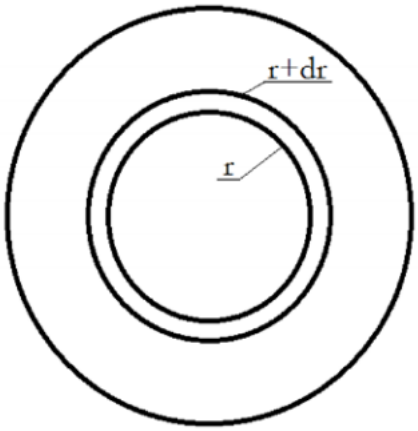

The cross section of an arbitrary infinitesimally thin shell within the simplified neonatal body. An energy balance taken around such a shell is equivalent to the energy balance taken around any point encompassed by the shell.

FIGURE - 8

Convective heat transfer is written as a function, Q, multiplied by the volume of the shell.

$$Convective\ HT = Q * V$$

Convective heat transfer is typically treated as a function of the surface area of the system. The model of convective heat transfer within the body is discussed later.

Radiative heat transfer is described as function R multiplied by the surface area (A) of the shell. Net radiative heat exchange is the difference of this product evaluated at the inner and outer layer of the shell. The is expresses as:

$$Radiative\ HT = (R * A)_{r+dr} - (R * A)_r$$

Fourier's Law describes conductive heat transfer and is:

$$J = -k * \nabla T$$

where J is conductive heat flux, k is thermal conductivity, and ∇T is the three dimensional temperature gradient. ∇T simplifies to a derivative of temperature with respect to radial position, recalling the assumption that temperature does not vary with longitudinal position.

$$J = -k * \frac{dT}{dr}$$

The difference in Fourier's Law multiplied by the surface area of the shell evaluated at the outer and inner surface of the shell gives the rate of heat entering and leaving the shell via conductive heat transfer.

$$Conductive\ HT = \left(-k * \frac{dT}{dr} * A\right)_{r+dr} - \left(-k * \frac{dT}{dr} * A\right)$$

Substituting the generation and consumption term and heat transfer terms into the energy balance equation and re-writing the equation in partial differential notation gives:

$$\frac{\partial(m * C_P * T)}{\partial t} = \left(-k * \frac{\partial T}{\partial r} * A\right)_{r+dr} - \left(-k * \frac{\partial T}{\partial r} * A\right)_r + (R * A)_{r+dr} - (R * A)_r + Q * V + B * V$$

Density, heat capacity, and volume are assumed to be independent of time. Re-writing the mass of the shell as the product of volume and density and dividing by the common volume term gives:

$$\rho * C_P \frac{\partial(T)}{\partial t} = \frac{\left(-k * \frac{\partial T}{\partial r} * A\right)_{r+dr} - \left(-k * \frac{\partial T}{\partial r} * A\right)_r}{V} + \frac{(R * A)_{r+dr} - (R * A)_r}{V} + Q + B$$

Re-writing A and V in terms of r and the length of the cylindrical body (L) and factoring out constant common monomials from the radiative and conductive heat transfer terms gives:

$$\rho * C_P \frac{\partial(T)}{\partial t} = \frac{2 * \Pi * L * \left(\left(-k * r \frac{\partial T}{\partial r}\right)_{r+dr} - \left(-k * r \frac{\partial T}{\partial r}\right)_r + (R * r)_{r+dr} - (R * r)_r\right)}{\Pi * (r + dr)^2 * L - \Pi * r^2 * L} + Q + B$$

Cancelling out common factors. The difference in conductive and radiative heat transfer at the inner and outer surface of the shell is re-written in differential form, recognizing that dr is infinitesimally small.

$$\rho * C_P \frac{\partial(T)}{\partial t} = \frac{1}{r} * \frac{\partial}{\partial r}\left(-k * r \frac{\partial T}{\partial r}\right) + \frac{1}{r} * \frac{\partial}{\partial r}(R * r) + Q + B$$

The above equation (Bio heat equation) is an energy balance that is generalizable to the entire simplified body. However, the abrupt changes in tissue type that occur along the radial direction causes discontinues in the energy balance taken around the entire body. This is addressed by applying a separate energy balance equation to the core, bone, muscle, connective, fat, and skin tissue separately. Integrating the final form of the energy balance within each tissue group gives the spatial and temporal temperature profile within the simplified neonatal body.

The following subsections expand on the terms Q and R. Terms describing convective and radiative heat exchange with the surroundings and evaporative heat loss from the skin are also described in the following sections.

➢ CONVECTIVE HEAT TRANSFER

The sum of the terms described in this subsection make up the function Q. Note that heat exchange coefficients between the skin and the environment are only included in Q when the energy balance is evaluated at the surface of the skin.

Heat exchange between tissue and blood: Pennes proposed a function describing convective heat transfer between a unit volume of tissue and blood in the microvasculature. This equation is widely used in the literature. Its general form is:

$$B_{micro} = \omega_{bl} * \rho_{bl} * c_{bl} * (T_{ar} - T_v)$$

where B_{micro}, is heat exchange between the tissue and blood in the capillaries per unit volume of tissue, ω_{bl} is basal blood perfusion rate through the tissue per unit volume of tissue, ρ_{bl} is the density of blood, c_{bl} is the heat capacity of blood, T_{ar} is the temperature of arterial blood entering the tissue, and T_v is the temperature of venous blood flowing out of the tissue element.

The temperature of blood is assumed to equilibrate with the temperature of the tissue before the blood exists the tissue element. This assumption was proposed by Pennes and supported in an analysis done by Chen. Applying this assumption to the heat exchange equation gives:

$$B_{micro} = \omega_{bl} * \rho_{bl} * c_{bl} * (T_{ar} - T)$$

Temperature of arterial blood entering the core tissue is set equal to the weighted average of the temperature of blood exiting the other tissue groups. The temperature of arterial blood entering tissue groups other than the core is set equal to the average temperature of the core tissue. Heat transfer due to bulk blood flow is not considered. Basal blood perfusion is assumed to be constant for a given tissue type.

Convective heat transfer with the surroundings: Convective heat exchange occurs between the skin and the surrounding air over half of the BSA (the surface area of the skin not covered by the blanket). An expression describing rate of heat transfer between the skin and bulk air is as follows;

$$C_{surr} = h * (T_s - T_\infty) * 0.50 * BSA$$

where C_{surr} is the heat flux secondary to convective heat transfer with the surrounding air, h is the overall heat transfer coefficient, T_s is the value of temperature at the skin surface, and T_∞ is the temperature of the bulk air.

There is no forced flow of air and bulk air temperature is assumed constant at 33 °C. Others measured the overall heat transfer coefficient pertaining to convective heat exchange between a nude neonate mannequin and stagnant air in an incubator environment to be 4.94 W/m2 -K [3]. This value is assumed to be constant.

➢ RADIATIVE HEAT TRANSFER

The sum of the terms described in this subsection make up the function R. In each circumstance, it is assumed that all the radiative energy absorbed by the skin takes on the form of heat. R includes terms describing blue light absorption and radiative heat exchange with the environment when the energy balance is evaluated at the surface of the skin.

Blue light absorption: The following integral quantifies blue light absorbed by the skin:

$$R_b = \int_{\lambda_i}^{\lambda_f} (I * \alpha(\lambda, \theta, \varphi)) d\lambda$$

where R_b is energy flux, I is spectral irradiance and α is monochromatic absorptivity of skin written as a function of the wavelength of incident light (λ), polar angle of incidence (θ), and azimuthal angle of incidence (ϕ). The blue light source emits radiation in the spectrum bounded by λ_i and λ_f.

The following equation relates absorptivity to reflectance (γ) and transmittance (τ):

$$1 = \alpha(\lambda, \theta, \varphi) + \tau(\lambda, \theta, \varphi) + \gamma(\lambda, \theta, \varphi)$$

Assuming that transmittance of blue light through the skin is negligible allows the absorption integral to be re-written as:

$$R_b = \int_{\lambda_i}^{\lambda_f} I * (1 - \gamma(\lambda, \theta, \varphi))d\lambda$$

It is assumed that the skin reflects blue light diffusely. This is expressed as:

$$\gamma(\lambda, \theta, \varphi) \approx \overline{\gamma(\lambda)} \; for \; all \; \theta \; and \; \varphi$$

Anderson and Parrish used an integrating sphere to measure diffuse reflectivity as a function of wavelength in the blue spectrum. Nielsen et al. modeled diffuse reflectivity of skin in the blue spectrum for different concentrations of cutaneous melanin. Their model is consistent with the measurements done by Anderson and Parrish. Reflectivity of skin (7.5% melanin) is written as a function of wavelength in the spectrum of 430-490 nm using predications made by Nielsen et al. This correlation is:

$$\overline{\gamma(\lambda)} = 9 * 10^{-6} * \lambda^2 - 0.0074 * \lambda + 1.6589$$

where wavelength is expressed in units of nm. This function is substituted into the absorption integral, and a definite integral is taken from 430 to 490 nm:

$$R_b = \int_{430\ nm}^{490\ nm} I * \left(1 - (9 * 10^{-6} * \lambda^2 - 0.0074 * \lambda + 1.6589)\right)d\lambda$$

Evaluating the integral while treating spectral irradiance as a constant gives:

$$R_b = I * 50.28$$

Recalling that blue light is incident on the top half of the neonate, the total heat entering the skin

$$R_B = \frac{BSA}{2} * I * 50.28$$

via absorption of blue light radiation (RB) is:

Radiation emitted by the surroundings: Radiation emitted by the plastic walls of the incubator and the blanket is absorbed by and heats the skin. The following integral quantifies the radiation emitted by the wall and the blanket and absorbed by the skin per unit surface area of skin:

$$R_{surr} = \int_0^{\infty} (M_{surr} * \alpha(\lambda, \theta, \varphi)) d\lambda$$

where R_{surr} is energy flux and M_{surr} is monochromatic emissive power of the walls and blanket. Skin absorptivity is assumed constant over the domain of wavelength while evaluating this integral. This is discussed later in this subsection. Applying this assumption to the absorption integral gives:

$$R_{surr} = \alpha * \int_0^{\infty} M_{surr}\, d\lambda$$

It is assumed that the black body model reasonably approximates the radiation emitted by the plastic walls and blanket. Given this, the integral of monochromatic emissivity over the domain of wavelength is equal to the Stefan-Boltzmann law.

$$R_{surr} = \alpha * \sigma * T_{\infty}^4$$

where T_{∞} is the temperature of the walls and blanket and σ is the Stefan Boltzmann constant. T_{∞} is set to 33 °C and constant, as mentioned before.

Integrating Planck's Law over the infrared (IR) region shows that 99% of the radiation emitted by a black body at 33 °C is within the IR band. Measurements of skin absorptivity are limited to a narrow band of wavelengths, and there is no outstanding model of skin absorptivity in the IR region. Given this, absorptivity is assumed to be one and constant. This assumption should be revisited when more empirical data is available. Applying this assumption gives:

$$R_{surr} = \sigma * T_{\infty}^4$$

The incubator walls and the blanket circumscribe the neonate body, and a view factor of one is assumed. The total heat entering the neonate as radiation emitted by the walls and blanket ($R_{surr,total}$) is:

$$R_{surr,total} = BSA * \sigma * T_{\infty}^4$$

Radiation emitted within the body and at the surface of the skin: Radiative heat transfer occurs within the body and at the surface of the skin. Assuming that radiation emitted by all tissue types is diffuse, the following integral gives the radiative heat emitted at each point within the body per unit area:

$$R_t = \int_0^{\infty} (\epsilon_{\lambda} * P(\lambda, T)) d\lambda$$

where R_t is flux, ϵ_{λ} is monochromatic emissivity and P(λ,T) is Planck's Law as a function of wavelength and temperature within the body.

Sanchez et al. measured the monochromatic emissivity of skin to be nearly one in the IR region from 3000 to 14000 nm and near constant. Others obtained similar values [22]. Given these findings, it is assumed that one approximates the emissivity of skin throughout the IR band.

Furthermore, over 99% of radiation emitted by a black body at a temperature of 33-39 °C exists within the IR band. Given this, it is assumed that the Stefan-Boltzmann Law reasonably approximates the total radiative power emitted by the neonatal skin.

Unfortunately, similar measurements of emissivity in other tissue types are not available in the literature. Given this, the model assumes that all tissue types emit like a black body.

Applying these assumptions and evaluating the integral over the domain of wavelength gives the Stefan-Boltzmann Law:

$$R_t = \sigma * T^4$$

➢ HEAT EXCHANGE DUE TO EVAPORATION OF WATER

Evaporative heat loss from the surface of the skin (E_{sk}) is the sum of heat lost due to water diffusing through the skin (E_{diff}) and vaporization of secreted sweat (E_{sw}).

$$E_{sk} = E_{diff} + E_{sw}$$

Attempts to model sweat production as a function of temperature in the neonate body are not widespread in the literature, and this model does not consider evaporation of sweat. The value of Ediff is calculated using the following formula from Gage, Stolwijk, and Nishi research. This is mathematically expressed as:

$$E_{sk} = E_{diff} = w_{diff} * \kappa * h * (P_{sk} - \phi_a * P_a) * F_{pcl}$$

where w_{diff} is a dampness factor equal to 0.06, κ is a proportionality constant equal to 2.2 °C/mmHg, h is the overall heat transfer coefficient previously used to describe convective heat exchange between the skin and bulk air, P_{sk} is vapor pressure of water at skin temperature in mmHg, φ_a is the relative humidity, P_a is vapor pressure at bulk air temperature in mmHg, and F_{pcl} is the permeation efficiency of water through clothes, equal to 1 in the current assessment of a nude neonate.

The air in the incubator is saturated with water (relative humidity is one). P_a is equal to 37.7 mmHg and constant, recalling the assumption that bulk air temperature is constant at 33 °C. The Antoine equation approximates the value of P_{sk} in units of mmHg as a function of mean skin temperature ($T_{skin,avg}$) in units of °C. This is:

$$P_{sk} = 10^{8.07 - \frac{1730.63}{233.43 + T_{skin,avg}}}$$

Substituting the Antoine equation into the formula for evaporative heat loss through the skin and multiplying this by the BSA of the neonate gives the rate of heat loss due to diffusion of water through the skin.

$$E_{sk} = BSA * w_{diff} * \kappa * h * \left(10^{8.07 - \frac{1730.63}{233.43 + T_{skin,avg}}} - \phi_a * P_a\right)$$

V. MODEL SOLUTION

➢ DISCRETIZATION

In computation world, discretization is the process of transferring continuous functions, models, variables, and equations into discrete counterparts. This process is usually carried out as a first step toward making them suitable for numerical evaluation and implementation on digital computers.

Discretization methods are used to chop a continuous function (i.e., the real solution to a system of differential equations in CFD) into a discrete function, where the solution values are defined at each point in space and time. Discretization simply refers to the spacing between each point in your solution space

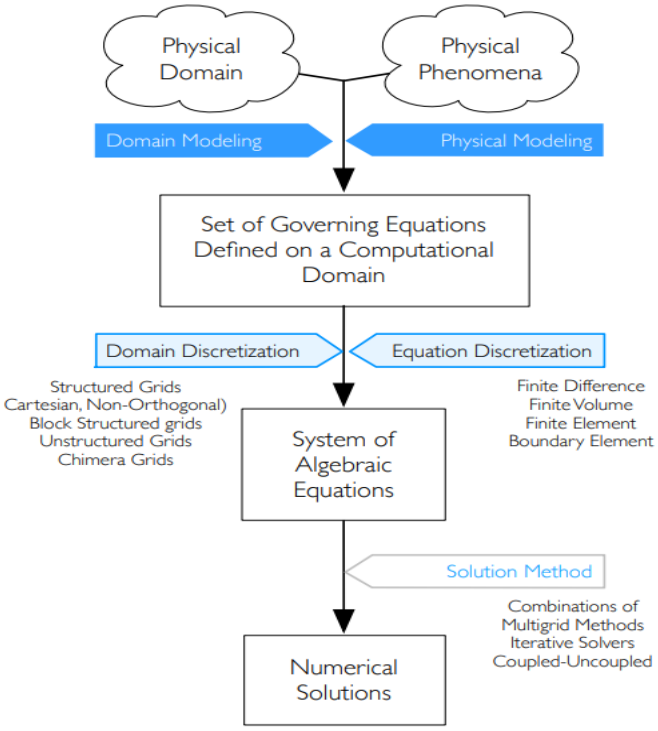

FIGURE – 9

➢ FINITE VOLUME METHOD

The Finite volume method (FVM) is a widely used numerical technique. The fundamental conservation property of the FVM makes it the preferable method in comparison to the other methods, i.e., FEM, and finite difference method (FDM). The FVM transforms the set of partial differential equations into a system of linear algebraic equations.

Firstly, it transforms and integrates the PDEs into balance equations over an element. The process incorporates the changing of the surface and volume integrals into discrete algebraic relations over elements as well as their surfaces using an integration quadrature of a specified order of

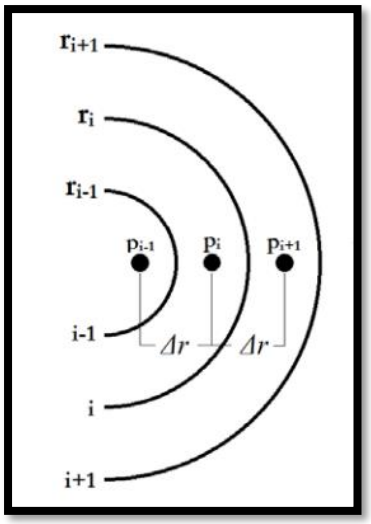

FIGURE – 10

accuracy. This will result in a set of semi-discrete equations. Secondly, in this next step, the interpolation profiles are chosen to estimate the variation of the variables within the element and relate the surface values of the variables to their cell values and thus transform the algebraic relations into algebraic equations. In regards to the two steps in the FVM process, your approximation selection affects the overall accuracy of the subsequent numeric.

The energy balance presented in the previous section is numerically integrated using the finite volume method. This technique is applied in other temperature models of the human body and to other heat and fluid transport problems. The general treatment is developed here and applied separately to each tissue group inside the neonate body.

The general form of the finite volume method applied to a cylindrical body begins by discretizing the cylinder into n number of equally spaced finite concentric shells.

The shells are numbered from 1 to n in the order they extend away from the centre of the cylinder. The symbol i is an integer between 1 and n and denotes an arbitrary shell in the series. The symbol r_i denotes the radius of the circle that bounds the outer perimeter of i_{th} shell. The symbol p_i denotes a point that lies midway between the inner and outer bounds of the $_{ith}$ shell in the radial direction. The width of each shell is equal to Δr. Figure on left side below illustrates this discretization, using a half the cylinder for better visualisation.

A half cylinder discretized into n number of uniform thin concentric shells. The shells are numbered from 1 to n in the order they extend outwards in the radial direction. The variable Δr is the width of each shell. The i_{th} shell is an arbitrary shell in the series. The variable r_i represents the outer radius of the i_{th} shell, and the variable pi represents the midpoint of the i_{th} shell in the radial direction.

The solution of the energy balance taken around the i_{th} shell is developed and is generalizable to all finite elements in the discretized body. Figure aside gives a local view of the i_{th} shell.

The i_{th} shell and its corresponding radius and midpoint. Shells adjacent to the i_{th} shell are shown. The midpoint of each shell is a distance Δr from the midpoint of the adjacent shell in both directions. An energy balance is developed around the i_{th} shell.

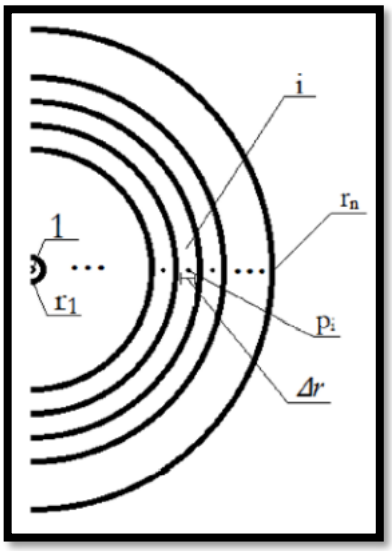

FIGURE - 11

The final form of the energy balance presented in the Model Development section is:

$$\rho * C_P \frac{\partial T}{\partial t} = \frac{1}{r} * \frac{\partial}{\partial r}\left(-k * r \frac{\partial T}{\partial r}\right) + \frac{1}{r} * \frac{\partial}{\partial r}(R * r) + Q + B$$

A definite double integral is taken over the time interval $[t_i, t_f]$ and the volume of the i_{th} shell.

$$\int_{V_{i-1}}^{V_i}\int_{t_i}^{t_f}\left(C_P * \rho * \frac{\partial T}{\partial t}\right) dtdV$$
$$= \int_{V_{i-1}}^{V_i}\int_{t_i}^{t_f}\left(\frac{1}{r} * \frac{\partial\left(-k * r\frac{dT}{dr}\right)}{\partial r}\right) dtdV + \int_{V_{i-1}}^{V_i}\int_{t_i}^{t_f}\frac{1}{r} * \frac{\partial}{\partial \mathrm{r}}(R * r)\, dtdV + \int_{V_{i-1}}^{V_i}\int_{t_i}^{t_f} Q\, dtdV$$
$$+ \int_{V_{i-1}}^{V_i}\int_{t_i}^{t_f} B\, dtrdr$$

The volume of the thin shell is approximated as follows:

$$dV = dr * rd\theta * dz$$

This is substituted into the energy balance, the polar and azimuthal terms are cancelled out, recalling that temperature is independent of these dimensions, and the common r factor in the radiative and conductive terms are cancelled out.

$$\int_{r_{i-1}}^{r_i}\int_{t_i}^{t_f}\left(C_P * \rho * \frac{\partial T}{\partial t}\right) dtrdr$$
$$= \int_{r_{i-1}}^{r_i}\int_{t_i}^{t_f}\left(\frac{\partial\left(-k * r\frac{dT}{dr}\right)}{\partial r}\right) dtdr + \int_{r_{i-1}}^{r_i}\int_{t_i}^{t_f}\partial(R * r)\, dt + \int_{r_{i-1}}^{r_i}\int_{t_i}^{t_f} Q\, dtrdr$$
$$+ \int_{r_{i-1}}^{r_i}\int_{t_i}^{t_f} B\, dtrdr$$

It is assumed that temperature does not vary with respect to radial position within the finite shell. Applying this assumption, the spatial integral is evaluated for all terms aside from the conduction and radiation terms.

$$\frac{({r_i}^2 - {r_{i-1}}^2)}{2} * \int_{t_i}^{t_f}\left(C_P * \rho * \frac{\partial T}{\partial t}\right) dt$$
$$= \int_{r_i-1}^{r_i}\int_{t_i}^{t_f}\left(\frac{\partial\left(-k * r\frac{dT}{dr}\right)}{\partial r}\right) dtdr + \int_{r_{i-1}}^{r_i}\int_{t_i}^{t_f}\partial(R * r)\, dt + \frac{({r_i}^2 - {r_{i-1}}^2)}{2} * \int_{t_i}^{t_f} Q\, dt$$
$$+ \frac{({r_i}^2 - {r_{i-1}}^2)}{2} * \int_{t_i}^{t_f} B\, dt$$

Re-arranging:

$$\int_{t_i}^{t_f}\left(C_P * \rho * \frac{\partial T}{\partial t}\right)dt$$

$$= \frac{2}{({r_i}^2 - {r_{i-1}}^2)} * \int_{r_i-1}^{r_i}\int_{t_i}^{t_f}\left(\frac{\partial\left(-k * r\frac{dT}{dr}\right)}{\partial r}\right)dtdr + \frac{2}{({r_i}^2 - {r_{i-1}}^2)} * \int_{r_{i-1}}^{r_i}\int_{t_i}^{t_f}\partial(R * r)\,dt +$$

$$+ \int_{t_i}^{t_f} Q\,dt + \int_{t_i}^{t_f} B\,dt$$

The net rate of radiative heat entering the i_{th} shell is the radiative power emitted by the i-1 shell across r_i-1 and i+1 shell across r_i subtracted by the radiative power emitted by the i_{th} shell across both r_i-1 and r_i. Applying this gives:

$$\int_{t_i}^{t_f}\left(C_P * \rho * \frac{\partial T}{\partial t}\right)dt$$

$$= \frac{2}{({r_i}^2 - {r_{i-1}}^2)} * \int_{r_i-1}^{r_i}\int_{t_i}^{t_f}\left(\frac{\partial\left(-k * r\frac{dT}{dr}\right)}{\partial r}\right)dtdr + \frac{2}{({r_i}^2 - {r_{i-1}}^2)}$$

$$* \int_{t_i}^{t_f}\left(r_i * (R_{i+1} - R_i) - r_{i-1} * (R_i - R_{i-1})\right) + \int_{t_i}^{t_f} Q\,dt + \int_{t_i}^{t_f} B\,dt$$

The time integral of the partial derivative of temperature with respect to time is the difference in temperature at time t_f and the temperature at time t_i. Recalling that heat capacity and density are assumed constant, this gives:

$$C_P * \rho * \left(T|_{t_f} - T|_{t_i}\right)$$

$$= \frac{2}{({r_i}^2 - {r_{i-1}}^2)} * \int_{r_i-1}^{r_i}\int_{t_i}^{t_f}\left(\frac{\partial\left(-k * r\frac{dT}{dr}\right)}{\partial r}\right)dtdr + \frac{2}{({r_i}^2 - {r_{i-1}}^2)}$$

$$* \int_{t_i}^{t_f}\left(r_i * (R_{i+1} - R_i) - r_{i-1} * (R_i - R_{i-1})\right) + \int_{t_i}^{t_f} Q\,dt + \int_{t_i}^{t_f} B\,dt$$

The derivative of temperature with respect to radius at r_i is approximated as the difference between temperature at the point p_i+1 and the point pi divided by Δr. Similarly, the derivative of temperature with respect to radius at r_i-1 is approximated as the difference between temperature at point pi and the point p_i-1 divided by Δr. Applying this assumption and treating k as a constant, the spatial integral of Fourier's Law is evaluated:

$$C_P * \rho * \left(T|_{t_f} - T|_{t_i}\right)$$

$$= \frac{-2 * k}{({r_i}^2 - {r_{i-1}}^2)} * \int_{t_i}^{t_f}\left(r_i * \frac{T|_{p_{i+1}} - T|_{p_i}}{\Delta r} - r_{i-1} * \frac{T|_{p_i} - T|_{p_{i-1}}}{\Delta r}\right)dt + \frac{2}{({r_i}^2 - {r_{i-1}}^2)}$$

$$* \int_{t_i}^{t_f}\left(r_i * (R_{i+1} - R_i) - r_{i-1} * (R_i - R_{i-1})\right) + \int_{t_i}^{t_f} Q\,dt + \int_{t_i}^{t_f} B\,dt$$

The time integrals on the right-hand side of the equation are evaluated by taking explicit Riemann sum approximations. Applying this and re-writing the difference between t_f and t_i as Δt gives:

$$C_P * \rho * \left(T|_{t_f} - T|_{t_i}\right) = \frac{-2 * k * \left(\left(r_i * \frac{T|_{p_{i+1}} - T|_{p_i}}{\Delta r} - r_{i-1} * \frac{T|_{p_i} - T|_{p_{i-1}}}{\Delta r}\right) dt\right) * \Delta t}{(r_i{}^2 - r_{i-1}{}^2)} + \frac{2 * \Delta t * \left(r_i * (R_{i+1} - R_i) - r_{i-1} * (R_i - R_{i-1})\right)}{(r_i{}^2 - r_{i-1}{}^2)} + \Delta t * Q + \Delta t * B$$

This formula approximates the temporal temperature profile of the i_{th} shell. The accuracy of the approximation improves as n becomes larger and Δt becomes smaller.

The solution is applied to each volume element in the discretized system. The finite volume method is applied separately to the core, bone, muscle, connective, fat, and skin tissue to obtain the spatial-transient temperature profile in each tissue group. Special consideration must be taken when applying the approximate integral of the energy balance to the 1st and nth element in each tissue group.

For all tissue types aside from the skin, the nth shell is below and adjacent to a shell representing a different tissue type. Consequently, heat exchange across the upper bound of each nth shell is dependent on the temperature of the nth shell as well as the temperature of the 1st shell in the tissue group that lies above it. This is conversely true for the 1st element in each tissue group aside from the core tissue. The nth shell of the skin tissue lies at the interface of the body and the incubator environment. Conductive heat exchange between the skin and the blanket is dependent on the temperature of the nth shell of the skin and the constant temperature of the blanket. Conductive heat exchange between the blanket and the skin occurs over half of the outer lateral surface area of the skin.

➢ CONSIDERATIONS/LIMITATIONS

The model may exaggerate the effect of blue light absorption on core temperature. Assumptions made during the development of the model minimize heat sinks in the surroundings. The incubator walls and the blanket emit radiation like black bodies. It is assumed that the absorptivity of neonatal skin in the IR spectra is one. Moreover, the model minimizes thermal resistance within the body by assuming perfect thermal contact between different tissue groups and assuming that each element emits and absorbs radiation like a black body. Minimizing heat sinks favors accumulation of heat in the body and reducing thermal resistance between tissues facilitates distribution of this heat to the core tissue. These aspects of the model may cause the predicted rise in core temperature due to heat entering the body at the surface of the skin to be greater than that which occurs in the true physical system.

The accuracy of spatial temperature variation is limited in this model. Singularities are produced in the function that approximates the integral of the energy balance when n becomes too large. Radiative and conductive heat exchange in and out of each shell is proportional to the surface

area of the shell and independent of its volume. At larger values of n, the volume of each shell approaches zero. Concurrently, the surface area of each shell remains near constant and, thus, radiative and conductive heat transfer in and out of the shell remains finite. This skews the temperature of each shell toward infinity, causing the series approximation to diverge as t becomes larger. This effect occurs at earlier values of t in the nth shell of the skin tissue, which experiences large radiative and conductive heat fluxes imposed on it by the surroundings. To avoid this phenomena, the value of n must be one when the finite volume method is applied to the skin tissue and ≤2 when it is applied to the other tissue groups. This limits the number of discrete points within the body at which temperature can be approximated, reducing the accuracy of modeled spatial temperature variation.

➢ RESULTS

The value of n was set equal to 1 for the skin and 2 for the remaining tissue groups. The total time was set equal to 24 h (24*60*60 sec), the length of phototherapy in MATLAB programme. The average temperature of each tissue group was calculated at each time point. Solutions and plots were generated using MATLAB which comprises one main file and six function files corresponding to each tissue considered.

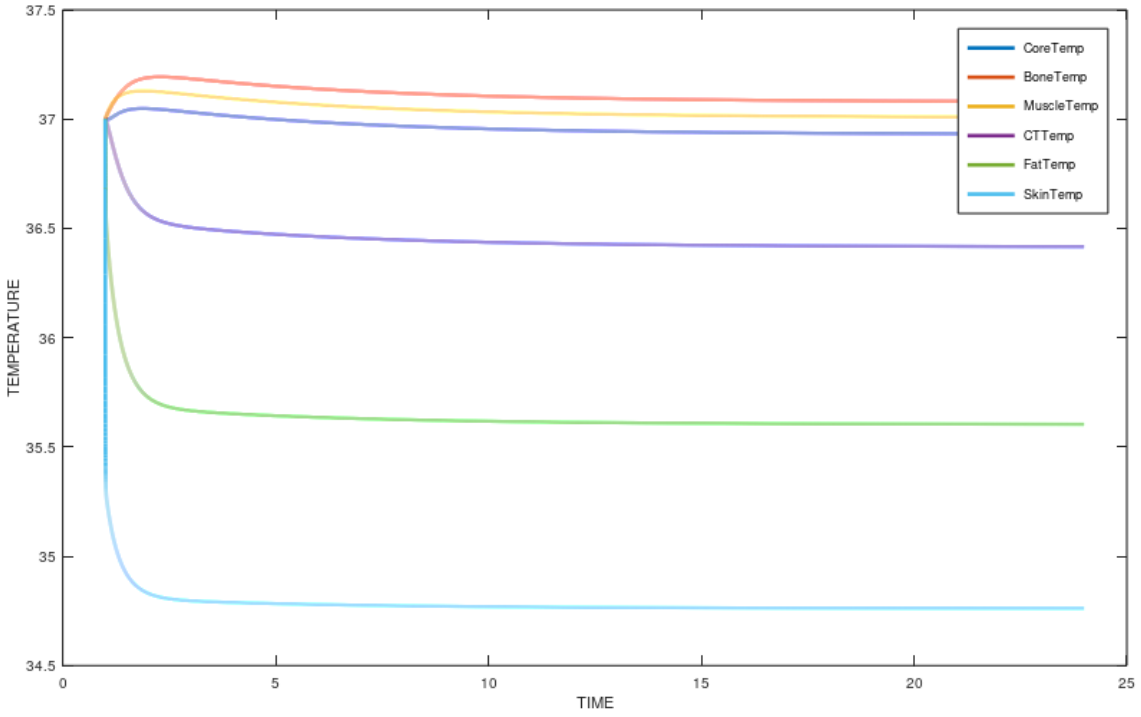

FIGURE 12

Average core temperature dropped during the first 15 min, rose for 45 min, dropped again and leveled off between 5-10 h to a near constant value of 36.9 °C for the remaining time. Average muscle and bone tissue temperatures rose during the first 5 h and then dropped. Both leveled off in the range of 37-37.3 °C. Average skin temperature dropped sharply from 37 to 34.4 °C within the first 3 h and leveled off at 34.4 °C for the remainder of time. Average fat and connective tissue temperatures both dropped sharply during the first 3 h and leveled off to 36.2 °C and 35.3 °C, respectively

Skin tissue temperature may have dropped sharply due to rapid heat exchange with the relatively cool environment. Direct heat exchange with the environment occurred only at the skin layer. Average core, fat, and connective tissue temperatures all dropped during the first 30 min. Fat and connective tissue are relatively close to the skin layer and may have experienced a sharp decline in temperature during the first hour due to conductive heat loss to the skin. Core tissue receives blood equilibrated to the temperature of skin, fat, and connective tissue. The initial drop in average core temperature may have occurred due to convective heat loss to the cold blood arriving from these peripheral tissue groups. The trend of average bone and muscle temperature contrasts with that exhibited by the other tissue groups. The muscle shell lies adjacent to and below the connective tissue shell, which exhibited an initial drop in temperature. However, basal metabolic heat production and basal blood perfusion rate are higher in muscle tissue relative to connective tissue. Moreover, the volume of the muscle tissue shell is over six times greater than that of the connective tissue shell. These factors may explain the initial rise in muscle temperature despite its proximity to the colder connective tissue. The bone shell lies under the warm muscle and above the core, relatively far from major sinks of heat. It is possible that bone tissue temperature rose initially and remained higher than that of other tissue groups due to its position

➢ CONCLUSION

Therefore, the results obtained through graphs represent variation of temperature in the neonate with respect to time (The graph is obtained by using certain parameters that are detected real-time and Hardware System may be installed with the Incubator itself.), by using which we can control the Intensive Blue Light Phototherapy by Real Time Monitoring of the neonate temperature in a detailed fashion rather than just checking the skin temperature.

VI. BIBLIOGRAPHY

- Neonatal Hyperbilirubinemia - Pediatrics - Merck Manuals Professional Edition
- Finite Element Method (FEM) vs. Finite Volume Method (FVM) in Field Solvers for Electronics | Advanc (cadence.com)
- Finite Volumes IMWE.pdf (udc.es)
- Chapter 05 The Finite Volume Method (aub.edu.lb)
- Sci-Hub | A finite volume method to compute the steady state temperature distribution in premature or newborn infants. ZAMM - Journal of Applied Mathematics and Mechanics / Zeitschrift Für Angewandte Mathematik Und Mechanik, 81(S3), 759–760 | 10.1002/zamm.200108115152 (sci-hub.st)
- Lecture Notes 3 ; Finite Volume Discretization of the Heat Equation (kth.se)
- https://www.youtube.com/watch?v=E9_kyXjtRHc&t=54s
- https://en.wikipedia.org/wiki/Computational_fluid_dynamics
- https://www.iue.tuwien.ac.at/phd/heinzl/node23.html
- https://www.iue.tuwien.ac.at/phd/heinzl/node4.html
- https://bioheat.umbc.edu/files/2015/07/Paper2007.pdf
- https://www.sciencedirect.com/science/article/pii/S0895717711008272
- https://www.worldscientific.com/doi/pdf/10.4015/S1016237202000139
- https://thermopedia.com/content/587/
- https://en.wikipedia.org/wiki/Convection%E2%80%93diffusion_equation#:~:text=The%20convection%E2%80%93diffusion%20equation%20is,two%20processes%3A%20diffusion%20and%20convection.
- https://engineer-educators.com/topic/3-heat-transfer-from-the-human-body/
- http://slu.adam.com/content.aspx?productid=117&pid=2&gid=19875
- https://scholar.rose-hulman.edu/cgi/viewcontent.cgi?article=1275&context=rhumj
- https://www.cfd-online.com/Forums/main/144808-matlab-code-finite-volume-method-2d.html